scientific data

OPEN

ANALYSIS

Cancer-specific association between Tau (*MAPT*) and cellular pathways, clinical outcome, and drug response

Maurizio Callari[1], Martina Sola[2], Claudia Magrin[2,3], Andrea Rinaldi[4], Marco Bolis[4,5,6], Paolo Paganetti[2,3,9] ✉, Luca Colnaghi[7,8,9] ✉ & Stéphanie Papin[2,9]

Tau (*MAPT*) is a microtubule-associated protein causing common neurodegenerative diseases or rare inherited frontotemporal lobar degenerations. Emerging evidence for non-canonical functions of Tau in DNA repair and P53 regulation suggests its involvement in cancer. To bring new evidence for a relevant role of Tau in cancer, we carried out an *in-silico* pan-cancer analysis of *MAPT* transcriptomic profile in over 10000 clinical samples from 32 cancer types and over 1300 pre-clinical samples from 28 cancer types provided by the TCGA and the DEPMAP datasets respectively. *MAPT* expression associated with key cancer hallmarks including inflammation, proliferation, and epithelial to mesenchymal transition, showing cancer-specific patterns. In some cancer types, *MAPT* functional networks were affected by P53 mutational status. We identified new associations of *MAPT* with clinical outcomes and drug response in a context-specific manner. Overall, our findings indicate that the *MAPT* gene is a potential major player in multiple types of cancer. Importantly, the impact of Tau on cancer seems to be heavily influenced by the specific cellular environment.

Introduction

It has been known for decades that the microtubule-binding protein Tau plays a role in causing debilitating neurodegenerative disorders[1]. Indeed, various rare autosomal dominant mutations in the *MAPT* gene encoding for the protein Tau cause frontotemporal lobar degeneration with Tau pathology (FTLD-Tau), which defines a small group of progressive frontotemporal dementia[2,3]. FTLD-Tau, together with Alzheimer's disease (AD), belongs to a group of tauopathies that are identified by the presence of an abnormal fibrillar form of hyperphosphorylated Tau protein inside the cells[4,5]. Subcellular distribution and activities of Tau that may not be related to its association with microtubules were recently described, including functions linking Tau to nucleic acids[6]. For instance, DNA lesions accumulate in the brains of *MAPT* knock-out (*MAPT* KO) mice or primary neurons[7,8]. Additionally, loss of heterochromatin is found in the brains of individuals with AD or in animal models of tauopathies[9–11]. Supporting this, Tau is present in the cell nucleus with a specific phosphorylation pattern[12] and binds to DNA in a sequence-independent manner[11,13,14]. Also, Tau depletion increases the sensitivity to DNA-damaging drugs in a xenograft model of breast cancer[15].

We reported that Tau depletion in cells recovering from acute DNA damage resulted in reduced initiation of programmed cell death because of P53 destabilization; an effect that was compensated by increased cellular senescence induction[16]. These findings suggest a molecular connection between Tau and P53 and a potential involvement in cancer[17], creating a possible link between neurodegeneration and cancer, two prevalent

[1]Michelangelo Foundation, Milan, Italy. [2]Laboratory for Aging Disorders, Laboratories for Translational Research, Ente Ospedaliero Cantonale, Bellinzona, Switzerland. [3]Faculty of Biomedical Sciences, Università della Svizzera Italiana, Lugano, Switzerland. [4]Institute of Oncology Research, Università della Svizzera Italiana, Bellinzona, Switzerland. [5]Computational Oncology Unit, Department of Oncology, IRCCS Istituto di Ricerche Farmacologiche 'Mario Negri', Milano, Italy. [6]Swiss Institute of Bioinformatics, Bioinformatics Core Unit, Bellinzona, Switzerland. [7]Division of Neuroscience, IRCCS San Raffaele Scientific Institute, Milan, Italy. [8]School of Medicine, Vita-Salute San Raffaele University, Milan, Italy. [9]These authors contributed equally: Paolo Paganetti, Luca Colnaghi, Stéphanie Papin. ✉e-mail: paolo.paganetti@eoc.ch; colnaghi.luca@unisr.it

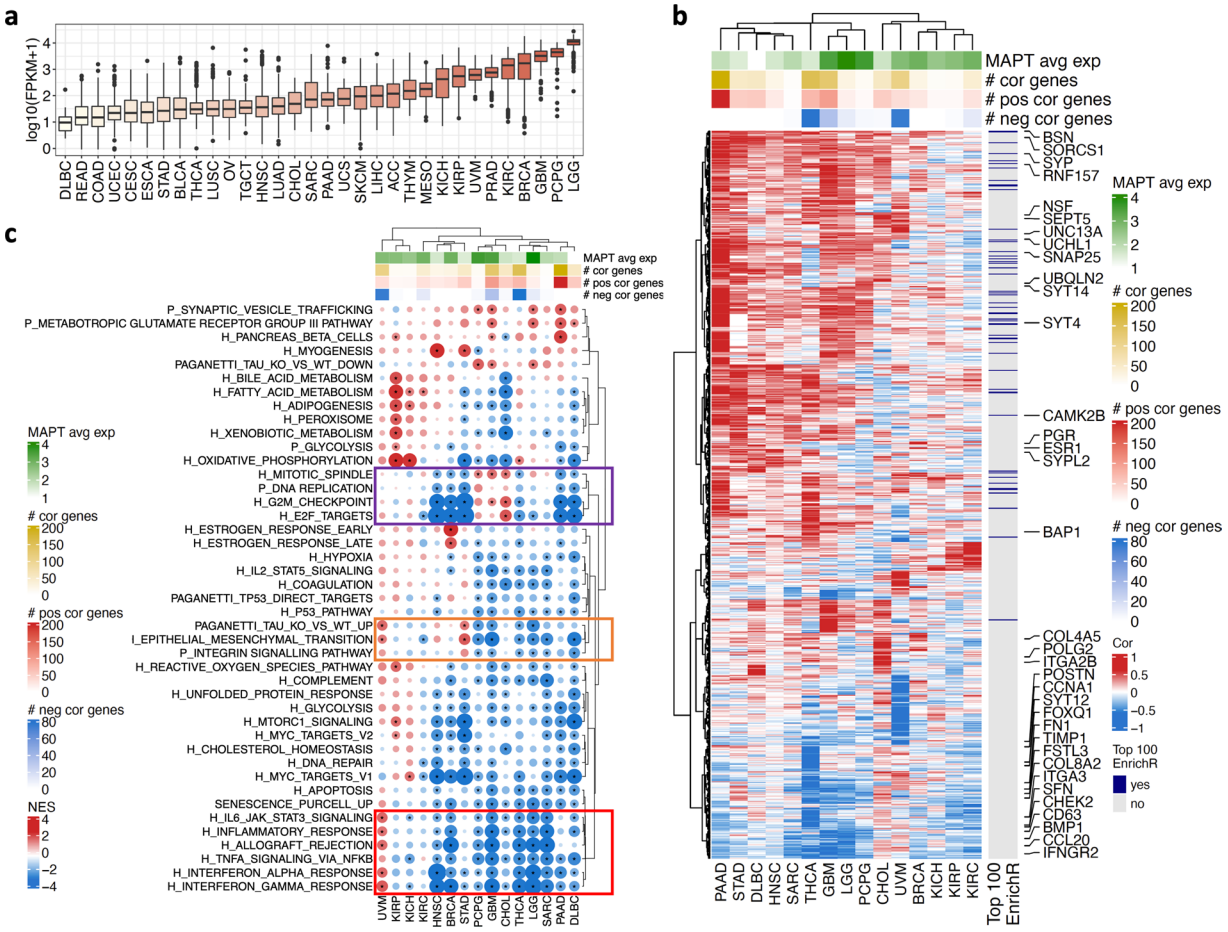

Fig. 1 Pan-cancer evaluation of *MAPT* expression and transcriptional associations. (**a**) *MAPT* expression in the TCGA according to cancer type; (**b**) Heatmap of 809 genes correlated with *MAPT* expression in at least one cancer type. Both genes and cancer types are ordered based on the hierarchical clustering of the correlation values. Genes in the list of top 100 genes co-expressed with *MAPT* according to EnrichR (ARCHS[4] dataset) are indicated. Selected genes are highlighted. For each cancer type, the average *MAPT* expression and the number of genes correlated with *MAPT* are shown. The whole pan-cancer results are reported in Figure S2. (**c**) GeneSet Enrichment Analysis on the genes ranked accordingly to their correlation with *MAPT* expression in each cancer type. A negative Normalised Enrichment Score (NES) means down-regulation of the geneset for high *MAPT* expression and vice versa for positive NES. Colored boxes indicate genesets commented in the text.

age-related human diseases[18]. Tau expression is correlated with the response to microtubule targeting drugs and other cancer treatments[17]. In the central nervous system (CNS) cancers neuroblastoma and glioma, Tau level correlates with survival[19,20]. Increased Tau protein is also associated with Isocitrate Dehydrogenase (*IDH1*) mutations in glioma (a likely driver of formation and development of this type of cancer[21]) and with improved prognosis and response to therapy. However, the comprehensive role of Tau in neoplastic conditions is still unclear.

Considering these initial reports supporting possible roles of Tau in cancer, we report herein the outcome of a set of pan-cancer analyses aimed at demonstrating the relevance of Tau in malignancies, identifying the genes and pathways associated with Tau, quantifying the impact of Tau expression on the clinical outcome and drug response, and exploring the possible interplay with P53. We mined the pan-cancer TCGA[22] dataset as well as the DEPMAP[23] resource, for a total of over 10000 clinical samples and over 1300 pre-clinical samples. Altogether, the obtained results support a critical and context-dependent role of Tau in cancer.

Results

***MAPT* co-expression analysis highlighted cancer-specific associations.** To shed light on the relevance of Tau in cancer, we evaluated *MAPT* gene expression values in 32 distinct cancer types mining the TCGA pan-cancer cohort. *MAPT* expression was highly variable, with brain glioblastoma multiforme (GBM), lower grade glioma (LGG), and neuroendocrine (pheochromocytoma and paraganglioma, PCPG) tumors showing the highest expression followed by breast cancer (BRCA) (Fig. 1a).

MAPT expression was next correlated with all expressed genes in each cancer type. The number of genes displaying a positive or negative correlation with *MAPT* expression was highly variable across cancers. We found correlated genes (absolute correlation threshold = 0.6) in 15 out of 32 cancer types (Figure S1a). The statistical

significance of the correlation was evaluated and corrected for multiple testing (Figure S1b). This confirmed that correlation values beyond the adopted threshold were largely significant in all types of cancer thanks to the large sample size available. The highest numbers of correlated genes were observed in pancreatic adenocarcinoma (PAAD), thyroid carcinoma (THCA), glioblastoma (GBM), and uveal melanoma (UVM) (Figure S1a). In some cases (e.g., PAAD), positive correlations were predominant, while negative correlations prevailed in THCA and UVM. We checked whether the total number of genes correlating with *MAPT* or the number of genes with a positive or a negative correlation depended on *MAPT* expression levels. Only a low-moderate correlation was observed in all cases (Figure S1c), suggesting only a weak link between the expression levels and the potential relevance of *MAPT* within cancer biological networks.

From the *MAPT*-all gene correlation analysis, we identified 809 genes with a significant correlation with *MAPT* in at least one cancer type (Fig. 1b and Figure S2). The unsupervised analysis of their correlation patterns identified 5 distinct cancer clusters (Figure S1d and Figure S2). Overall, tumor types tended to cluster according to their organ or apparatus of origin. Indeed, HNSC, ESCA, STAD, COAD, and READ were all members of cluster 2, GBM, LGG, and PCPG were the component of cluster 3 while KICH, KIRP, and KIRC all belonged to cluster 1. At the same time, in some instances, very different cancer types (e.g. BRCA and kidney cancer) could be members of the same cluster, indicating an overall similarity in the way genes correlated with *MAPT* expression (Figure S2). We intersected our list of genes with the top 100 genes co-expressed with *MAPT* according to EnrichR, which uses the ARCHS[4] dataset (see Methods). Fifty-two genes were included in the 809 identified in the TCGA (Fig. 1b and Figure S2). Considering that any kind of human tissue is included in ARCHS[4] and that the pan-cancer correlation highlighted substantial differences among cancer types, the overlap was remarkable.

In the 15 cancer types with significantly correlated genes, the correlation analysis was complemented with a GeneSet Enrichment Analysis (GSEA). For each cancer type, genes ranked by correlation with *MAPT* became the input of a GSEA to identify biological processes and pathways having a positive or negative correlation with *MAPT* expression (Fig. 1c). For example, a negative Normalised Enrichment Score (NES) indicates that a specific pathway or geneset tends to be under-expressed when *MAPT* expression is high. We evaluated the Cancer Hallmark collection[24], the PANTHER Pathway collection[25], and additional custom genesets. Indeed, in light of our previous findings showing that Tau stabilizes P53 and negatively modulates senescence in response to DNA damage[16], we include four additional genesets capturing senescence[26–29] or direct P53 target genes[30–33]. We also included a geneset containing the top 100 genes dysregulated in *MAPT* KO neuroblastoma cells[16,34] when compared to Tau-expressing neuroblastoma cells (Figure S1e).

For the way geneset enrichment analysis works, significant positive/negative NES could be observed even if no genes were beyond the 0.6 threshold (e.g., negative NES in PAAD) or, in some cases, no significant enrichment could be found even if single genes showed significant correlations (e.g., no negative NES in UVM) (Fig. 1c). Consequently, we considered the GSEA analysis as complementary to the single gene correlation analysis, with the aim of pinpointing the most interesting associations. Biological interpretation of the results highlighted both commonalities and cancer-specificity in the way *MAPT* expression relates to the tumor ecosystem transcriptomic profile. Genes involved in migration or epithelial to mesenchymal transition (EMT) (*ITGA2B*, *COL4A5*, *FSTL3*, *COL8A2*, *FN1*, *BMP1*, *TIMP1*, *FOXQ1*, *ITGA3*, *POSTN*, *CD63*) correlated with *MAPT* expression positively or negatively depending on the cancer type (Fig. 1b). Similarly, genesets related to these biological functions (INTEGRIN_SIGNALLING_PATHWAY and EPITHELIAL_MESENCHIMAL_TRANSITION) were also bi-directionally associated with *MAPT* according to the cancer type (Fig. 1c, o**range box** and Figure S3a). Our signature of upregulated genes in *MAPT* knock-out neuroblastoma cells (PAGANETTI_TAU_KO_VS_WT_UP) (Figure S1e) showed an analogous pattern of association. Coherently with the original experiment, a negative enrichment in brain tumors was observed.

An additional pathway showing a strong variation of the NES according to the cancer type was the OXIDATIVE-PHOSPHORYLATION pathway, which reflects mitochondrial activity. This pathway was negatively enriched in most cancer types with few exceptions: in tumors derived from the kidneys (KICH, KIRP), and to a lesser extent in UVM and THCA, it was strongly positively enriched.

Genesets related to inflammation (INTERFERONα_RESPONSE, INTERFERONγ_RESPONSE, IL6_JAK_STAT3_SIGNALING, TNF_SIGNALING_VIA_NFKB, INFLAMMATORY_RESPONSE, ALLOGRAFT_REJECTION) globally showed a negative enrichment in all but UVM cancer. The strongest negative enrichments were found in sarcoma (SARC), GBM, LGG, THCA, and BRCA (Fig. 1c, r**ed box**). *IFNGR2* and *CCL20* were among the significantly correlated genes related to these biological functions (Fig. 1b). Quite intriguing were the positive enrichments for the same inflammation-related genesets observed in UVM. Whilst in many cancer types increased infiltration by immune cells is generally associated with better prognosis, infiltrating immune cells are critical contributors of UVM malignancy progression[35]. This make the pair with the opposite association with *MAPT*, but further research would be needed to better unveil the modulatory role of Tau on the inflammatory microenvironment.

Negative enrichment was evident for one of the senescence genesets (SENESCENCE_PURCELL_UP[29]), possibly explained by the increase in the secretion of inflammatory mediators during cellular senescence[36], some of which are part of the geneset.

Cell cycle-related genesets (G2M_checkpoint, E2F_targets, DNA_REPLICATION, MITOTIC_SPINDLE) were mostly negatively correlated with *MAPT*, in particular in HNSC, BRCA, STAD, PAAD, and DLBC. A few exceptions, with opposite trends, were found for CHOL, PCPG, and GBM (Fig. 1c, v**iolet box, and** Figure S3b). Multiple genes related to DNA replication, repair, and cell cycle progression did show significant correlations, e.g. *CHEK2, SFN*, *POLG2*, *CCNA1*.

The two genesets related to P53 (P53_PATHWAY, PAGANETTI_TP53_DIRECT_TARGETS) were associated with *MAPT* expression with a similar pattern across the cancer types. Negative NES below −2 were observed for at least one of the two genesets in DLBC, GBM, PCPG, and THCA. Therefore, high expression of

MAPT leads to a reduced expression of P53 target genes in these cancer types. This is in line with our previous findings where the P53_PATHWAY was positively enriched upon Tau KO in neuroblastoma cells (Figure S1e), supporting an interplay between Tau and P53 further explored in the next section.

Among the 809 genes, we found multiple neuronal genes positively correlating with *MAPT* across most cancer types (e.g., *BSN*, *SORCS1*, *CAMK2B*, *SNAP25*, *SEPT5*, *UNC13A*, *UCHL1*, *NSF*, synaptophysins *SYP* and *SYPL2*, and synaptotagmins *SYT4*, *SYT12* and *SYT14*), some of which have been linked to AD. For example, *SORCS1* polymorphism is associated with AD[37], whereas CAMK2 dysregulation in the hippocampus of AD subjects may contribute to neurofibrillary tangle formation, synaptic degeneration, and memory deficits[38]. Consistent with the high number of neuronal genes correlated with *MAPT*, enrichment for the SYNAPTIC_VESICLE_TRAFFICKING geneset was detected, particularly in brain tumors and PAAD, confirming that *MAPT* expression is often associated with a wider activation of a neuronal transcriptional program in cancer. However, this is not ubiquitous across distinct cancer types and a tendency to negative correlation for the same set of genes was observed, for example, in KIRP (Fig. 1b,c and Figure S3c).

Some correlations and enrichments were highly cancer-specific. For example, this is the case for estrogen response genes (e.g., ESTROGEN_RESPONSE_EARLY) specifically enriched in BRCA, with *ESR1* and *PGR* highly correlated with *MAPT* in this cancer type. This was consistent with literature data demonstrating that estrogens regulate *MAPT* expression[39–41], supporting the robustness of the present analysis.

Finally, it is worth mentioning that genes involved in ubiquitination processes and linked to cancer were among the significantly correlated genes (*BAP1*, *RNF157*, *UBQLN2*).

In summary, *MAPT* expression levels are associated with major cancer hallmarks, with some commonalities across groups of cancer types but a high degree of tumor specificity, indicating that the biological networks that include *MAPT* are highly context-specific.

***MAPT* co-expression analysis highlighted P53-dependent associations.** Tau is mostly characterized as a microtubule-stabilizing protein and may influence cancer outcomes through this cellular function. However, we recently described a new role of Tau as a positive modulator of P53 stability in neuroblastoma cells[16]. Considering that P53 is mutated in half of the tumors, these findings propose a possible upstream influence of Tau in the cancer biology of P53, an influence that may lose its weight when P53 is mutated. We first evaluated *MAPT* expression in P53 wild type (WT) versus mutated tumors (Fig. 2a and Figure S4a). The expression of *MAPT* was significantly different in WT and P53-mutated tumors in four cancer types (BRCA, LGG, LIHC, PAAD). P53 mutations were additionally functionally grouped in truncating mutation/homozygous deletion (Truncating/HomDel) and Inframe/Missense mutations, which could have a distinct functional impact and, in this case, a distinct impact on *MAPT* expression (Fig. 2b and Figure S4b). We observed a highly significant decrease in *MAPT* expression for both mutation types in BRCA. In this cancer type, it has been shown that the expression of *MAPT* is associated with subtypes i.e., high in ER+ tumors, which have the lowest P53 mutation rate[42]. For LGG, PAAD, SARC, OV, HSCN, and LIHC, we observed a significant change in *MAPT* expression depending on the type of P53 mutation (Truncating/HomDel or Inframe/Missense) or compared to WT (Fig. 2b and Figure S4b).

Next, we separately delineated genes and pathways associated with *MAPT* expression in 19 cancer types with data from at least 20 tumors with mutated or WT P53 (Table S1). We searched for genes correlated with *MAPT* expression, separately for P53-mutated and WT tumors, and computed, for each cancer type, their correlation delta (Figure S5). Significant delta values i.e., absolute delta above 0.6, were found in 8 cancer types (READ, ESCA, PAAD, GBM, LGG, CESC, SARC, and KICH) and 514 genes had a significant delta in at least one cancer type (Fig. 2c, Figure S6, and Figure S7). For three cancer types i.e., CESC, ESCA, and READ, while no genes were significantly correlated with *MAPT* in the overall population (Figure S2), correlated genes emerged when stratifying for P53 status. In general, we observed a prevalence of positive delta i.e., higher correlation with *MAPT* in P53 mutant. This was particularly evident in READ, while a prevalence of negative delta was observed in KICH (Fig. 2c).

This analysis allowed us to highlight *MAPT*-gene correlations that strongly depended on the P53 status, identifying an additional pool of genes with a potential context-specific biological link with *MAPT* (Fig. 2c). Among them, MDM2, a key P53 antagonist, displayed a positive delta in seven out of eight cancers. The correlation between *MAPT* and *MDM2* was mostly negative in WT P53 tumors whereas mutant P53 tumors showed either a loss of correlation (GBM, LGG) or a correlation in the opposite way (READ, CESC, SARC) (Figure S6). Since a loss of correlation with mutated P53 could indicate a role for Tau upstream of P53, and considering that MDM2 is the main E3 protein ubiquitin ligase and inhibitor of P53, the Tau-MDM2 link suggested a possible mechanism for the modulatory role of Tau on P53. Notably, we found that Tau binds and modulates MDM2[43]. Alternatively, considering that P53 activation of *MDM2* transcription[44] is lost when P53 is mutated, this may explain the reduced *MAPT-MDM2* correlation when P53 is mutated in LGG and GBM.

A single gene: *NMI* (N-Myc and STAT interactor), showed a weak positive delta in all eight cancer types with a negative correlation between *MAPT* and *NMI* in WT P53 tumors in all eight cancer types and a decrease of the correlation in P53 mutant tumors. NMI is an interferon-inducible protein participating in various cellular activities and has been involved in the process of tumorigenesis and tumor progression[45].

The associations of *MAPT* expression with genes encoding for proteins involved in proliferation, EMT, and inflammation were very variable among cancers (Fig. 2c). As an example, the correlations with *CDKL3* and *FBXO31*, two genes encoding for proteins involved in proliferation, showed similar behavior in READ and ESCA, with a negative correlation in WT P53 tumors and a positive correlation in P53 mutant tumors, whereas quite opposite correlation changes were observed in GBM, CESC, and KICH. In the EMT dataset, some correlations with *MAPT* varied similarly in a defined cancer type whereas they changed oppositely in another cancer type. As an example, negative correlations existed with *LOXL3* and *ZNF326* in P53 WT tumors

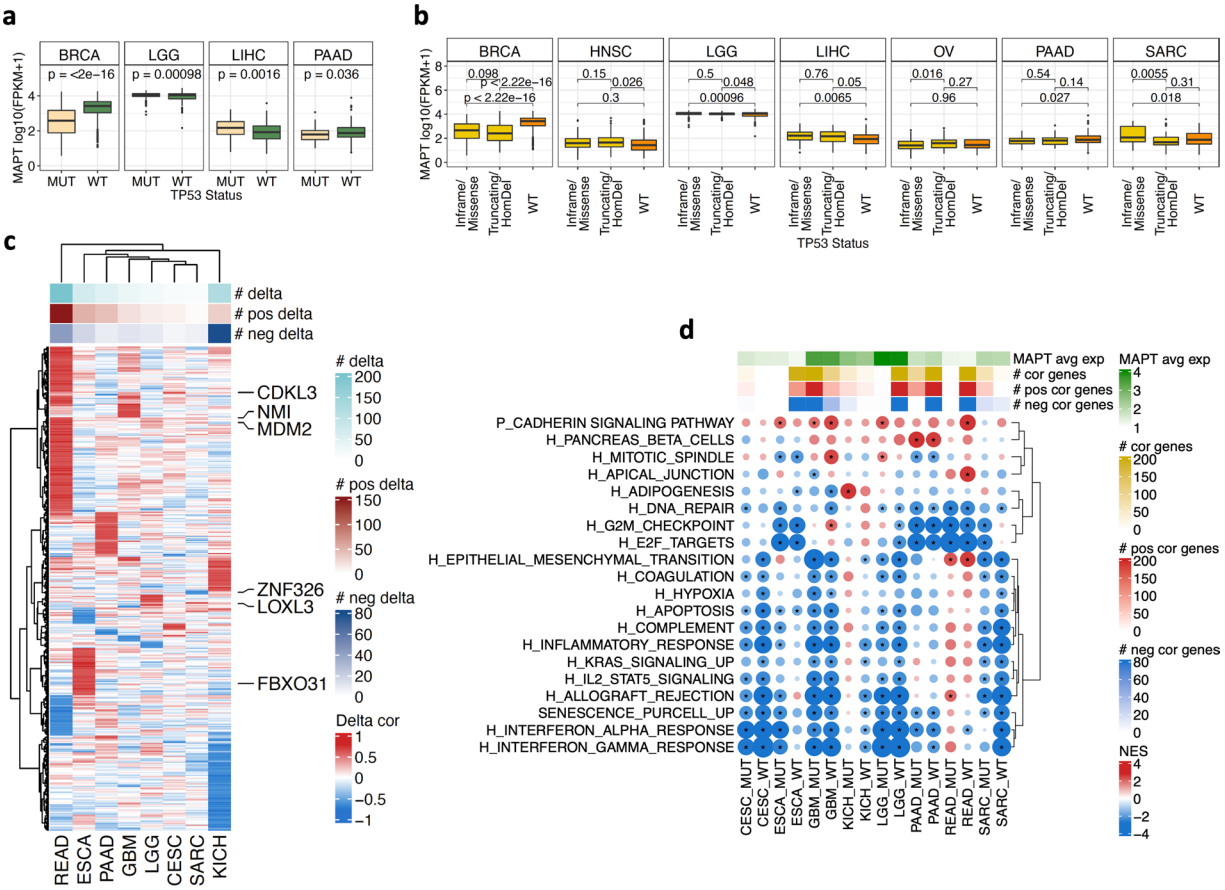

Fig. 2 Pan-cancer evaluation of MAPT expression and transcriptional associations stratified by P53 status. (**a**) Expression of *MAPT* in *TP53* WT and *TP53* MUT tumors. Boxplots for the cancer types with significant differences (two-sided Student's t-test) are reported. The full analysis is reported in Figure S4a. (**b**) Expression of *MAPT* in tumors with WT P53 or with either a Truncating/HomDel mutation or an Inframe/Missense mutation in *TP53*. Boxplots for the cancer types with at least one significant difference (two-sided Student's t-test) are reported. The full analysis is reported in Figure S4b. (**c**) Heatmap of 514 genes with an absolute delta correlation above 0.6 in P53 WT vs P53 MUT tumors for at least one cancer type. The correlation analysis was performed only for cancer types that included > 20 patients for each P53 status. Eight cancer types had more than one gene with a significant delta and are shown. An extended version of the results is reported in Figures S5 and S6. (**d**) GeneSet Enrichment Analysis on the genes ranked accordingly to their correlation with Tau expression within each cancer type and separately for P53 wild-type and P53-mutant tumors. Genesets with an absolute delta enrichment above 2.3 are reported for the eight cancer types shown in (**b**).

but were strongly decreased in mutant P53 tumors; whereas in SARC, *MAPT* negatively correlated with *LOXL3* and positively with *ZNF326*, this was reversed in mutant P53 tumors (Fig. 2c and Figure S6).

In the eight cancer types with significant delta values, we complemented the gene level analysis with a GSEA on genes ranked according to the correlation with *MAPT* in P53 WT and P53 mutated tumors for the same eight cancers. Genesets with a significant delta NES are shown in Fig. 2d. Several enrichments are affected by P53 status, positively or negatively, and in a cancer-specific manner. For CESC, ESCA, GBM, and LGG, the association of *MAPT* with inflammatory pathways was not changed according to P53 status. On the contrary, IFN-related genesets had a negative association with *MAPT* expression in KICH and SARC overall population (Fig. 1c). However, after stratifying by P53 status, we found that such an association was stronger and significant only in P53 WT tumors. Also, the association of cell cycle genesets with *MAPT* was affected by P53 status in some cancer types. Indeed, the positive association with *MAPT* in GBM (G2M_CHECKPOINT) was limited to the P53 WT tumors; similarly, the negative association in LGG was limited to P53 WT tumors. In SARC, no association with cell cycle genesets was observed overall (Fig. 1c); however, a significant negative association was present in P53 mutant tumors (Fig. 2d).

These data indicated that *MAPT*-correlated modulation of several biological processes depended on the status of P53 for some cancer types, possibly informative for an upstream or downstream effect of Tau on P53 cancer biology.

Cancer-specific and P53-dependent associations of *MAPT* with patients' survival. After exploring genes and pathways linked to *MAPT* expression, we thoroughly analyzed the association of *MAPT* with

	ALL - Univariate			ALL - Multivariate			TP53 WT - Univariate			TP53 WT - Multivariate			TP53 MUT - Univariate			TP53 MUT - Multivariate		
Cancer	N	HR	P	N	HR	P	N	HR	P	N	HR	P	N	HR	P	N	HR	P
ACC	79	0.97	0.9418	77	0.76	0.5226												
BLCA	423	1.22	0.1753	179	1.59	0.0516	203	1.36	0.1597	**96**	**2.17**	**0.0380**	214	1.10	0.6409	79	1.20	0.5982
BRCA	**1203**	**0.30**	**0.0000**	**1017**	**0.31**	**0.0000**	**706**	**0.28**	**0.0000**	**587**	**0.32**	**0.0006**	385	1.33	0.3062	342	0.89	0.7177
CESC	296	1.30	0.2976	104	1.06	0.9208	242	1.16	0.5879	82	0.94	0.9370						
CHOL	45	0.80	0.6037	38	0.97	0.9553												
COAD	**470**	**1.64**	**0.0161**	408	1.20	0.4606	179	1.49	0.2661	156	0.77	0.5815	**220**	**2.06**	**0.0123**	183	1.59	0.1692
ESCA	196	1.04	0.8781	149	0.88	0.6761							169	1.13	0.6239	128	0.92	0.7954
GBM	167	0.97	0.8589	167	0.98	0.9053	100	1.04	0.8620	100	1.04	0.8558	57	1.05	0.8723	57	1.10	0.7623
HNSC	**562**	**1.43**	**0.0080**	182	1.68	0.0511	153	1.24	0.4567	105	1.57	0.2252	378	1.33	0.0666	133	1.49	0.2048
KICH	89	1.50	0.5212	37	1.19	0.9264												
KIRC	**604**	**0.44**	**0.0000**	293	0.61	0.0598												
KIRP	320	1.26	0.4477	59	2.44	0.1254												
LGG	**529**	**0.24**	**0.0000**	**529**	**0.34**	**0.0000**	**260**	**0.19**	**0.0000**	**260**	**0.33**	**0.0018**	**260**	**0.29**	**0.0002**	**260**	**0.36**	**0.0030**
LIHC	**418**	**1.46**	**0.0209**	262	1.22	0.3672	269	1.15	0.5209	172	1.01	0.9699	123	1.69	0.0712	91	1.37	0.3972
LUAD	563	0.77	0.0734	393	0.90	0.5329	265	0.67	0.0653	190	0.87	0.5777	284	0.87	0.4713	194	0.98	0.9510
LUSC	548	1.17	0.2538	443	1.07	0.6559	66	1.23	0.5628	65	1.43	0.3424	443	1.18	0.3084	362	1.15	0.4394
MESO	86	1.17	0.5212	57	1.05	0.8766												
OV	308	1.19	0.2809	308	1.19	0.2751												
PAAD	182	0.68	0.0663	85	1.10	0.7659	65	0.61	0.2075	61	0.68	0.4290	107	0.71	0.1802	53	0.92	0.8283
READ	164	1.00	0.9918	147	0.87	0.7511							100	2.87	0.1105	91	1.99	0.3267
SARC	265	1.10	0.6614	265	1.22	0.3725	149	1.08	0.7880	149	1.10	0.7365	108	1.12	0.7379	108	1.49	0.3118
SKCM	463	1.03	0.8556	357	1.35	0.1224	298	1.43	0.0786	**222**	**1.99**	**0.0053**	59	0.97	0.9368	48	1.22	0.6909
STAD	421	1.12	0.4535	392	1.01	0.9357	211	1.11	0.6138	197	0.99	0.9665	205	1.06	0.8130	190	0.99	0.9705
THCA	571	2.11	0.1356	324	3.57	0.1182												
UCEC	**553**	**1.94**	**0.0041**	**553**	**2.01**	**0.0026**	**326**	**2.56**	**0.0173**	**326**	**2.74**	**0.0109**	**197**	**1.91**	**0.0350**	**197**	**1.89**	**0.0397**
UCS	56	1.87	0.0830	56	1.84	0.0925												
UVM	80	2.66	0.1031	55	0.27	0.1568												

Table 1. Univariate and multivariate Cox survival analysis for each cancer type in all samples and stratified by P53 status.

cancer survival. Univariate Cox regression analysis was performed for each cancer in the overall population, and separately for P53 WT and mutant subgroups. Then, we applied a multivariate Cox regression analysis adjusting for tumor size, lymph node status, metastatic status, and expression of the *AURKA* gene as a reporter of the proliferation process, associated with survival in multiple cancers (Table 1).

A high expression of *MAPT* was associated with a worse prognosis in COAD, HNSC, LIHC, and UCEC in the univariate analysis, and only for UCEC in the multivariate analysis. In contrast, high *MAPT* expression was associated with a better prognosis in BRCA, KIRC, and LGG in the univariate analysis and for BRCA and LGG in the multivariate analysis. These data suggested that the (positive or negative) correlation of *MAPT* expression with survival was independent of the other prognostic factors for BRCA, LGG, and UCEC. For some examples, we found a P53 status-dependent association between *MAPT* expression and cancer survival. This was the case for BRCA where the *MAPT*-survival correlation was lost for the P53 mutant cases. In other cancer types, for example, LGG, the positive association of *MAPT* with survival occurred in both P53 WT and P53 mutant cohorts. Similarly, for UCEC, the negative association appeared independent of the P53 status. Finally, the negative association between *MAPT* and survival detected for COAD appeared limited to the P53 mutant cases. The most significant Kaplan-Meier curves showing *MAPT* association with survival are shown in Fig. 3a, and the complete analysis is reported in Figure S8.

Since the variable association with survival in different cancer types, we evaluated whether this could be related to a change in the biological network associated with *MAPT* expression. To this aim, we searched for an association between *MAPT*-gene correlation values and *MAPT* hazard ratios from the Cox univariate analysis. We found associations between the way *MAPT* correlated with certain genes and the way it was associated with survival (Fig. 3b). Among the top genes, some encode for fundamental structural proteins such as a collagen subunit (*COL5A3*) or an extracellular matrix glycoprotein (*THSD4*), which play a weighty role in EMT and migration processes[46,47]. Other genes (e.g., *FBXL16*, *PDIA6*, *PPIB*) are involved in processes of protein folding and/or degradation, and their possible implication in tumorigenesis has been reported[48–50] (Figure S9). A similar analysis was done to link hazard ratios with GSEA enrichment scores but no geneset was identified (Fig. 3c).

***MAPT* expression and association with drug response in pre-clinical models.** Our analysis to chart the relevance of *MAPT* in cancer continued in pan-cancer pre-clinical data. We analyzed the CRISPR DEPMAP data collection (https://depmap.org/portal/) for the cell viability after *MAPT* KO across cell lines from

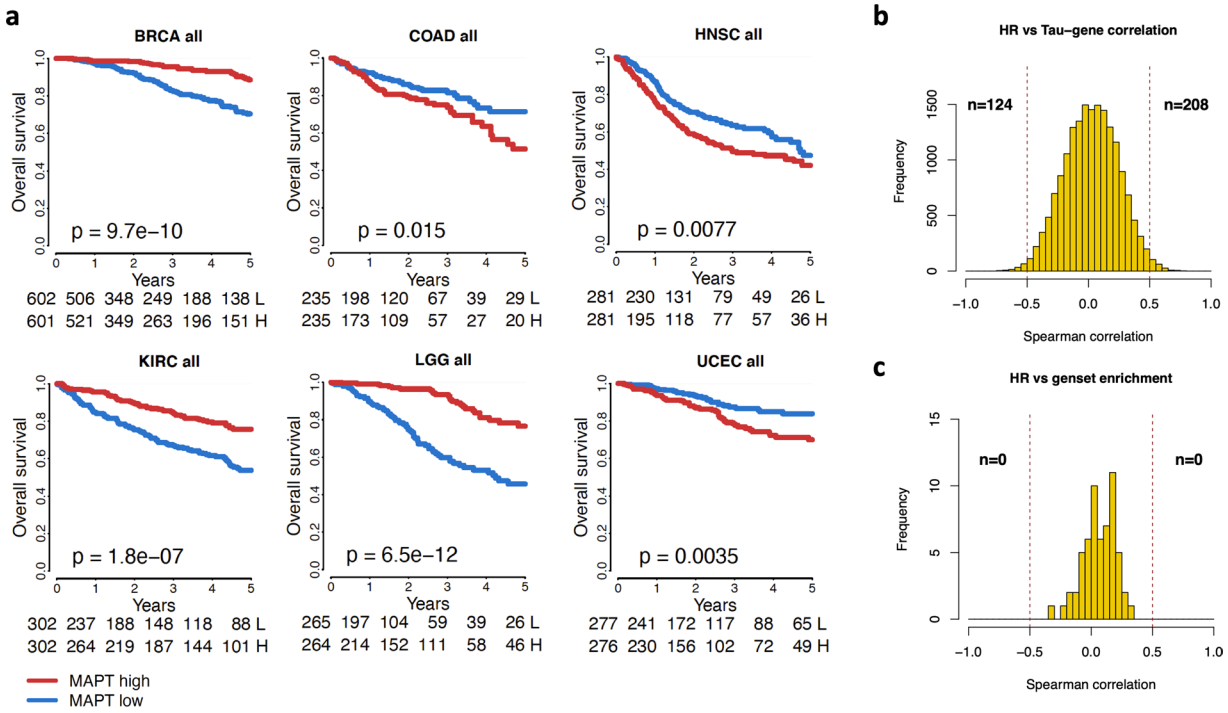

Fig. 3 *MAPT* cancer-specific association with survival.(**a**) Selected Kaplan-Meier curves showing the association between *MAPT* and survival in 6 cancer types. P-value obtained by log-rank test. (**b**) For each gene, its correlation with *MAPT* across all cancer types was correlated with hazard ratios (univariate Cox analysis) for the same cancer types. Histogram shows the distribution of values obtained. Number of genes with a correlation >0.5 or <-0.5 are indicated. (**c**) Same analysis as in (b) but computed correlating NES for each geneset with hazard ratios.

29 different cancer types. The impact of *MAPT* KO on viability was cancer-specific but overall, a decrease in viability is prevalently observed, except for rhabdoid cell lines (Fig. 4a).

For the DEPMAP cell line data collection, we also correlated *MAPT* expression with drug response, where the area under the drug response curve (AUC) with values ~0 indicated drug sensitivity and values ~1 indicated drug resistance. First, we evaluated *MAPT* expression across cancer cell lines grouped by cancer type. The highest expression was observed in neuroblastoma and bone cancer (Fig. 4b). The availability of proteomic data in the DEPMAP dataset for a subset of cell lines allowed us to determine that *MAPT* transcript and Tau protein strongly correlated (cor = 0.62), indicating that evaluating mRNA expression is informative for Tau protein levels (Fig. 4c).

After data filtering, we evaluated 121 drugs in 22 cancers (Fig. 4d, e). The associations involved multiple drug families and were largely specific to the cancer type. Of note, drugs tended to cluster based on their target or mechanism. A negative correlation between *MAPT* expression and resistance to several drugs with various modes of action is detected in pancreatic, uterine, and mainly bone cancer-derived cell lines, whereas predominantly positive correlations were found in cell lines derived from other cancers. In bone cancer cell lines, high *MAPT* expression was observed to be linked with a positive response to kinase inhibitors (Aurora, PI3K), HDAC inhibitors as well as DNA damaging drugs. The most significant correlations were found with belinostat, an HDAC inhibitor mainly used for the treatment of peripheral T cell lymphoma[51], and with talazoparib, a PARP inhibitor used for the treatment of advanced breast cancer with germline BRCA mutation[52]. Both drugs are now in clinical studies in bone cancers[53,54]. In liver cancer cell lines, *MAPT* expression was negatively associated with resistance to bleomycin, a DNA-damaging drug approved for squamous cell head and neck cancer, Hodgkin's lymphoma, and testicular carcinoma[55]. In uterine cancer cells, high *MAPT* expression correlated with sensitivity to kinase inhibitors. A very good correlation resulted with GSK2126458, a PI3K/mTOR inhibitor with broad antitumor activity in preclinical and clinical studies[56]. Resistance to MEK inhibitors correlated positively with *MAPT* for cell lines derived from breast and lung cancer, and negatively for skin-derived cell lines. Association between *MAPT* expression and resistance to kinases inhibitors was also detected in lymphocytes (PI3K) and bone and uterus-derived cancer cell lines (Aurora kinase). Surprisingly, response to microtubule-targeting drugs did not show a very strong correlation with *MAPT* expression. While cells derived from uterine and bone cancers were the ones with the higher number of drugs correlated with *MAPT* expression, only a few drugs did the same for cell lines derived from tumors affecting tissues such as the CNS, colorectal, upper aerodigestive, blood, and esophagus. Cell lines from the cervix, soft tissue, lung, breast, peripheral nervous system, liver, lymphocyte, and kidney showed a *MAPT* correlation with the response to several drugs.

Overall, these data highlighted that *MAPT* expression may represent an informative predictor of drug response in multiple cancer types.

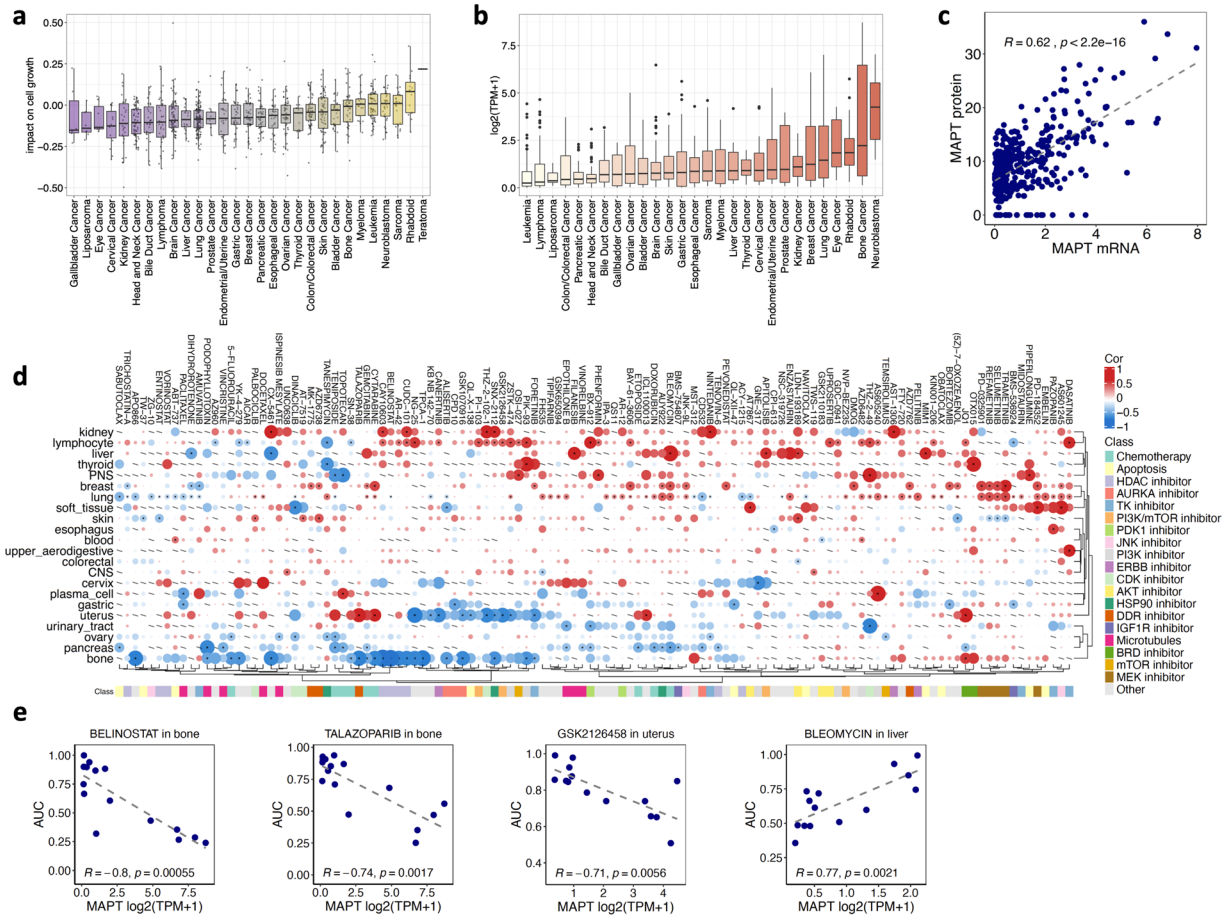

Fig. 4 *MAPT* expression, essentiality, and association with drug response in pre-clinical models. (**a**) Cell viability after *MAPT* KO in the CRISPR DEPMAP dataset. Viability scores are normalized such that nonessential genes have a median score of 0 and independently identified common essentials have a median score of −1. (**b**) *MAPT* expression in the DEPMAP cell line dataset according to the cancer type. (**c**) Correlation of *MAPT* gene expression with Tau protein (sum of three isoforms) in the DEPMAP cell line dataset. (**d**) Heatmap summarizing the correlations between *MAPT* expression with drug response quantified as area under the drug response curve (AUC). (**e**) Selected scatterplots of *MAPT*-drug response association.

Discussion

To strengthen the emerging evidence for the role of *MAPT* in cancer, we performed a pan-cancer *in silico* analysis to define the landscape of pathways, genes, and drug treatments associated with *MAPT* expression. We report a significant association between *MAPT* and cell proliferation, inflammation, and EMT-related genes. These genes are part of cellular pathways fundamental for tumor initiation, progression, and heterogeneity[57], with the latter also having a key link with the tumor microenvironment. In particular, interferons and inflammation-related genes could suggest a link between *MAPT* expression and inhibition of anti-tumor immune response, with possible therapeutic implications given the fast-paced clinical implementation of the immunotherapy[58].

Interestingly, we observed a positive pan-cancer correlation of *MAPT* with a large set of neuronal genes. Some of these have a clear role in AD pathology[38], further connecting these two very different human conditions that are usually considered to be inversely associated[59]. These findings are also in line with evidence suggesting that cancer cells recapitulate features of neuronal cells and reactivate mechanisms of neural differentiation and/or plasticity to achieve progression[60]. Tumors may also be able to stimulate their innervation during cancer progression[61] and to invade already existing nerves along the perineural space[62]. Both cancer cells and nerve fibers secrete factors that favor rapid growth of both, making the neural-epithelial interaction a mutually beneficial process[63]. In addition, cancer cells themselves may acquire brain-like properties as an adaptation for brain colonization. For example, i) breast-to-brain metastatic tissue and cells display phenotypes and metabolism similar to that of neuronal cells[64] and ii) malignant melanoma exhibits cytological characteristics of nerve cells[65]. Interestingly, all the neuronal genes and the neuronal pathway coming up as strongly associated with *MAPT* expression were not detected in the P53 status analysis, suggesting that the association of *MAPT* with this neuronal pathway in several cancer types is independent of P53 status.

Genes modulated after *MAPT* KO in neuroblastoma cells (PAGANETTI_TAU_KO_VS_WT) were associated with *MAPT* expression in multiple cancer types. Importantly, genes downregulated after *MAPT* KO had a positive association with *MAPT* in brain tumors (GBM, PCPG, LGG) and vice versa for upregulated genes.

Thus, gene modulation after *MAPT* KO in the neuroblastoma cell line was recapitulated in the *MAPT*-gene correlation analysis in brain cancer clinical samples. This supports the relevance of the pre-clinical model and the potential of our analysis to identify biological networks linked to *MAPT* expression.

Considering our recent findings[16], we aimed to characterize the possible interplay between *MAPT* and P53 in cancer. *MAPT* expression levels were different according to P53 status in some cancer types. In BRCA, the lower *MAPT* expression observed in P53 mutant tumors may be explained by the fact that P53 mutations are found more in ER-, PR- basal carcinoma (~88%) when compared to ER+, PR+ luminal tumors (~26%) in which *MAPT* is upregulated by ER/PR[42]. A negative association between *MAPT* expression and expression of P53 target genes was detected in many cancer types, particularly in brain tumors. This agreed with the data obtained in neuroblastoma cells depleted of Tau (Figure S1e). However, a positive association was found in BRCA, KIRP, and UVM, unveiling some tissue specificity in this relationship.

Furthermore, we stratified the pan-cancer *MAPT*-gene correlation analyses by P53 status i.e., mutated or WT. The analysis revealed that the association of *MAPT* expression with cell cycle, inflammation, and EMT varies not only according to the cancer type but, in some instances according to P53 status. Additional hints on the connection between Tau and P53 came from the *MAPT-MDM2* correlation pattern. *MDM2* is the main E3 protein ubiquitin ligase and antagonist of P53 and had a high delta correlation in READ, driven by a negative correlation with *MAPT* in P53 tumors.

Our study expanded a previous report[19], based on an older version of the TCGA dataset, on the association of *MAPT* expression with patient survival. In that study, a positive correlation between *MAPT* expression and survival in glioma, breast cancer, kidney clear cell carcinoma, lung adenocarcinoma, and pheochromocytoma/paraganglioma was described. While the log-rank test was applied in the previous study[19], our analytical approach was based on the Cox regression model that we deemed more appropriate when running univariate and multivariate breakdowns. Doing so, we also identified a negative correlation in uterine cancer in a multivariate analysis. Moreover, we also separated low-grade glioma from glioblastoma to reveal a positive correlation only in the former, thereby providing additional information compared to previous studies grouping these two cancer types[66]. We found a positive correlation between *MAPT* expression and survival in breast cancer, in line with previous studies[67–71]. The association remained significant in the multivariate analysis, indicating independence from other prognostic factors. Estrogen and progesterone directly modulate the *MAPT* promoter[40,72], explaining our observation of a strong positive correlation of *MAPT* with estrogen pathways and partially explaining the association with better survival.

The observation that *MAPT* is associated positively or negatively with survival depending on the cancer type, led us to the hypothesis that this could be linked with the distinct biological networks we found associated with *MAPT*. While a complex picture emerged, we identified genes for which their correlation with *MAPT* and *MAPT* hazard ratio were associated, partially confirming our hypothesis. Most of these genes encode either for structural proteins (COL5A3), components of the extracellular matrix (THSD4) or contributing to protein folding and/or degradation (FBXL16, PDIA6, PPIB). They are involved in proliferation, EMT, adhesion, and migration processes[46–50], thereby strengthening the observed association between *MAPT* expression and proliferation and EMT processes. Interestingly, the protein encoded by the best-associated gene, FBXL16, stabilizes C-MYC by blocking its ubiquitination and promotes cancer cell proliferation and migration[73].

In our characterization of *MAPT's* role in cancer, we also investigated its association with drug response in cell lines derived from 22 different cancer types. The best-described association between Tau and drug response was with drugs targeting microtubules, such as taxanes. As a microtubule-binding protein, it has been proposed that Tau could compete with taxanes in the binding with microtubules. Low Tau is associated with a better response to taxanes in breast[72] ovarian[74,75], gastric[76], prostate[77], and non-small-cell lung cancer[78]. Nevertheless, some studies came to the opposite conclusion and some Paclitaxel trials did not confirm the predictive value of Tau determination[67–69]. Our study did not detect a strong association between *MAPT* expression and microtubule-targeting drugs. Negative correlations were detected with Paclitaxel in gastric, plasma cell, and lung-derived lines, with podophyllotoxin in bone and pancreas-derived cells whereas a positive correlation is found with filanesib in liver-derived cells. Our study highlights, however, a strong association of *MAPT* expression with two other classes of cancer drugs, HDAC inhibitors, and several kinase inhibitors. A recent study suggests a possible predictive role of Tau expression in regards to HDAC inhibitors[11], however, the association of *MAPT* with sensitivity to kinases (PI3K, Aurora) inhibitors in bone-derived cells is a new finding. Osteosarcoma is a frequent type of pediatric bone cancer for which, despite many advancements in diagnostic technology, no efficient therapy approach has been identified because of the high metastasis rate and drug resistance[79]. PI3K and Aurora kinase, both involved in mitosis and cell proliferation, are overexpressed in osteosarcoma, and represent promising targets for osteosarcoma treatment[80,81]. The identification of *MAPT* as a predictive marker for response to these inhibitors may open, once validated in human biopsies, a new therapeutic perspective. We also detected strong positive and negative correlations between *MAPT* expression and drug responses in uterus-derived cell lines. Positive correlations are mainly detected with chemotherapy agents, whereas negative correlations are detected for Aurora and PI3K inhibitors, for example. Aurora kinase is frequently overexpressed in ovarian cancer and its expression has a prognostic value. Therefore the Aurora kinase family has evolved as a potential target for precision medicine in cancer[82]. In the last decade, several Aurora kinase inhibitors have been developed and tested in several cancer types. Two recent clinical trials with different Aurora kinase inhibitors have shown activity in epithelial ovarian and clear-cell ovarian cancer[82]. We may speculate that Tau interferes with Aurora kinase both at the level of the microtubule network and also at the level of P53, as multiple pieces of evidence underly a crosstalk between Aurora kinase and P53[82]. The presence of several correlations between high *MAPT* expression and response to drugs with various modes of action in bone and uterus-derived cells indicate that *MAPT* expression may represent a powerful marker to predict response to combination therapies in bone and uterine cancer. Strikingly, a positive correlation between *MAPT* and response to several MEK

inhibitors is found in breast and lung-derived lines. This could be particularly relevant in lung cancer where MEK inhibitors in combination with chemotherapy are highly significant for improving clinical efficacy and causing a delay in the occurrence of drug resistance[83].

A possible limitation of our study is that correlation-based analyses cannot imply causation. Experiments would be required to unveil the detailed molecular mechanisms, but this would be possible only in one or a few pre-clinical models, with known limitations in being representative of clinical tumors. On the contrary, in our analysis we were able to interrogate the largest molecularly characterized pan-cancer cohorts that, with over 10 000 clinical specimens from 32 distinct cancer types and over 1000 pre-clinical samples, could better recapitulate the clinical disease and clinical heterogeneity, offering the opportunity to gain a comprehensive overview of the putative role of Tau in cancer, fostering and providing guidance for further research and validations. Finally, relevant subtypes have been described for some cancer types (e.g. BRCA and COAD) and alterations of *MAPT* expression could be attributed partially to the presence or prevalence of such subtypes, but this was not directly addressed in this study.

Altogether, we described how several pathways and genes are associated with *MAPT* expression in all main cancer types. We comprehensively assessed the association between *MAPT* and survival, and the possible link with P53 status, and we present evidence that *MAPT* expression may affect the response to multiple classes of therapeutics.

Materials and Methods

Datasets. *TCGA Dataset analysis.* The Cancer Genome Atlas pan-cancer dataset was downloaded at https://gdc.cancer.gov/about-data/publications/pancanatlas (Downloaded files: EBPlusPlusAdjustPANCAN_IlluminaHiSeq_RNASeqV2.geneExp.tsv and clinical_PANCAN_patient_with_followup.tsv). A total of 11069 samples from 32 different cancer types were present in the dataset. The 'acronym' indicating the cancer type was not available for 213 samples that were excluded from the present study. Only genes with log10(FPKM + 1) average expression above 0.5 and standard deviation above 0.2 in at least one cancer type were kept for downstream analysis (n = 17646). Tau expression was correlated with the expression of all genes using Spearman correlation, as implemented in the stats (v. 3.5.0) R base package.

P53 mutations and CNA status also downloaded from the GDC portal were grouped to identify WT and MUT samples and to distinguish functionally distinct groups according to the scheme in Table S2.

DEPMAP Dataset analysis. *MAPT* CRISPR KO, gene expression, proteomic and drug-response pan-cancer cell line data from the Dependency Map initiative were downloaded from https://depmap.org/portal/. (Downloaded files from version 21Q1: CCLE_expression.tsv, protein_quant_current_normalized.csv, sanger-dose-response.csv, sample_info.csv; from PRISM Repurposing 19Q4: primary-screen-replicate-collapsed-logfold-change.csv). Cancer types with more than one cell line present in the gene expression dataset were included. Cell lines labelled as "Engineered" and "Fibroblast" were excluded. After this filtering, gene expression was available for 1320 cell lines from 28 cancer types. Drug response data were available for 692 of them, belonging to 22 cancer types. The area under the drug response curve (AUC), ranging between 0 (response) and 1 (resistance) was correlated with Tau expression for each cancer type. Spearman correlation was performed only when at least 10 cell lines were tested and at least two sensitives (AUC < 0.8) and two resistant (AUC > 0.8) were present. A total of 121 compounds tested in at least 11 of 22 cancer types were reported. Normalized mass spectrometry data across 375 cell lines[84] were used to evaluate the correlation between *MAPT* gene expression and Tau protein levels. All datasets after sample and/or feature filtering are made available as described in the Data availability section.

MAPT knock-out signature in neuroblastoma cells. RNA-Seq data derived from human neuroblastoma SH-SY5Y wild-type or KO for Tau (accession no. E-MTAB-8166) were downloaded from (https://www.ebi.ac.uk/biostudies/arrayexpress/studies/E-MTAB-8166?key=64a67428-adb9-4681-99c9-98910b78ed4c)[34]. The top 100 genes upregulated and the top 100 downregulated after *MAPT* KO generated two genesets (PAGANETTI_TAU_KO_VS_WT_UP and PAGANETTI_TAU_KO_VS_WT_DOWN respectively) included in the GSEA.

Data analysis. *Correlation analysis.* All statistical analyses were performed using R (v 4.2, platform: x86_64-apple-darwin17.0, running under macOS Big Sur 11.4). Association between two continuous variables (i.e. gene-gene expression) was quantified by Spearman's correlation analysis. Using the cor.test function, p-values were estimated and Benjamini-Hochberg corrected using the p.adjust function.

Identification of top 100 genes co-express with MAPT using EnrichR. Using EnrichR[85] (https://maayanlab.cloud/Enrichr/) we identified the top 100 genes co-expressed with MAPT in the ARCHS4 human tissue RNA-seq dataset. Genes were overlapped with our list of 809 genes that we found correlated with *MAPT* in at least one cancer type.

Unsupervised analysis. Cancer types were clustered based on the *MAPT*-gene correlation profile. The ConsensusClusterPlus method[86] was implemented using the K-means algorithm and Euclidean distance. The optimal number of clusters was established based on the delta are plot (Figure S1d).

GeneSet Enrichment Analysis (GSEA). A custom list of genesets to be tested was created as follows. The HALLMARK geneset collection was downloaded from the MSigDB (https://www.gsea-msigdb.org/gsea/msigdb/, v 7.1). The genesets related to the PANTHER classification system[87] were downloaded from https://maayanlab.cloud/Harmonizome/dataset/PANTHER+Pathways. Four further genesets were added, three

related to senescence (SENESCENCE_HERNANDEZ-SEGURA, SENESCENCE_PURCELL, SENESCENCE_CASELLA)[26,27,29], one collecting P53 direct targets (PAGANETTI_TP53_DIRECT_TARGET)[30–33] and PAGANETTI_TAU_WT_VS_KO described above. Correlation-ranked genes were tested for geneset enrichment using the gsea function from the *phenoTest* (v.1.28.0) R/Bioconductor package. Genesets with FDR < 0.1% and absolute NES > 2.3 in at least one cancer type were considered significant and reported. In the analysis stratified by P53 status, an absolute delta NES between P53 mutant and WT tumors above 0.6 was considered significant.

Selected PANTHER pathways were represented and overlaid with *MAPT*-gene correlation values in selected cancer types using the SBGNview (v. 1.10.0) R/Bioconductor package[88].

Survival analysis. Association with overall survival was performed as univariate or multivariate Cox regression analysis as implemented in the *survival* (v.3.1) R/Bioconductor package. The analysis was performed when at least 10 events (deaths) were present in the considered subset of cancer cases and when, in multivariate analysis, information for at least three of the four covariates (Size, Lymph node status, Metastatic status, AURKA gene expression) was available in at least 20 patients. P-value < 0.05 indicate a significant association. *MAPT* expression was dichotomized in high or low using the median expression as a cut-off.

Code availability

No custom algorithms have been developed in this study. Reference code related to the main analyses performed is available at https://github.com/mauricallari/MAPT

Data availability

Imported and filtered datasets used to generate the presented results are available on Zenodo (https://doi.org/10.5281/zenodo.8069665, https://zenodo.org/record/8069665)[34].

Received: 23 June 2023; Accepted: 5 September 2023;
Published online: 20 September 2023

References

1. Gao, Y. L. *et al.* Tau in neurodegenerative disease. *Annals of translational medicine* **6**, 175 (2018).
2. Shi, Y. *et al.* Structure-based classification of tauopathies. *Nature* **598**, 359–363 (2021).
3. Josephs, K. A. Rest in peace FTDP-17. *Brain: a journal of neurology* **141**, 324–331 (2018).
4. Goedert, M., Eisenberg, D. S. & Crowther, R. A. Propagation of Tau Aggregates and Neurodegeneration. *Annual review of neuroscience* **40**, 189–210 (2017).
5. Xia, Y., Prokop, S. & Giasson, B. I. "Don't Phos Over Tau": recent developments in clinical biomarkers and therapies targeting tau phosphorylation in Alzheimer's disease and other tauopathies. *Mol Neurodegener* **16**, 37 (2021).
6. Galas, M. C., Bonnefoy, E., Buee, L. & Lefebvre, B. Emerging Connections Between Tau and Nucleic Acids. *Adv Exp Med Biol* **1184**, 135–143 (2019).
7. Sultan, A. *et al.* Nuclear tau, a key player in neuronal DNA protection. *The Journal of biological chemistry* **286**, 4566–4575 (2011).
8. Violet, M. *et al.* A major role for Tau in neuronal DNA and RNA protection *in vivo* under physiological and hyperthermic conditions. *Frontiers in cellular neuroscience* **8**, 84 (2014).
9. Frost, B., Hemberg, M., Lewis, J. & Feany, M. B. Tau promotes neurodegeneration through global chromatin relaxation. *Nature neuroscience* **17**, 357–366 (2014).
10. Klein, H. U. *et al.* Epigenome-wide study uncovers large-scale changes in histone acetylation driven by tau pathology in aging and Alzheimer's human brains. *Nature neuroscience* **22**, 37–46 (2019).
11. Rico, T. *et al.* Tau Stabilizes Chromatin Compaction. *Frontiers in cell and developmental biology* **9**, 740550 (2021).
12. Ulrich, G. *et al.* Phosphorylation of nuclear Tau is modulated by distinct cellular pathways. *Scientific reports* **8**, 17702 (2018).
13. Qi, H. *et al.* Nuclear Magnetic Resonance Spectroscopy Characterization of Interaction of Tau with DNA and Its Regulation by Phosphorylation. *Biochemistry* **54**, 1525–1533 (2015).
14. Mansuroglu, Z. *et al.* Loss of Tau protein affects the structure, transcription and repair of neuronal pericentromeric heterochromatin. *Scientific Reports* **6**, 33047 (2016).
15. Rico, T. *et al.* Cancer Cells Upregulate Tau to Gain Resistance to DNA Damaging Agents. *Cancers* **15** (2022).
16. Sola, M. *et al.* Tau affects P53 function and cell fate during the DNA damage response. *Communications biology* **3**, 245 (2020).
17. Papin, S. & Paganetti, P. Emerging Evidences for an Implication of the Neurodegeneration-Associated Protein TAU in Cancer. *Brain sciences* **10** (2020).
18. Houck, A. L., Seddighi, S. & Driver, J. A. At the Crossroads Between Neurodegeneration and Cancer: A Review of Overlapping Biology and Its Implications. *Current aging science* **11**, 77–89 (2018).
19. Gargini, R., Segura-Collar, B. & Sánchez-Gómez, P. Novel Functions of the Neurodegenerative-Related Gene Tau in Cancer. *Frontiers in aging neuroscience* **11**, 231 (2019).
20. Zaman, S., Chobrutskiy, B. I. & Blanck, G. MAPT (Tau) expression is a biomarker for an increased rate of survival in pediatric neuroblastoma. *Cell cycle (Georgetown, Tex.)* **17**, 2474–2483 (2018).
21. Huang, L. E. Friend or foe—IDH1 mutations in glioma 10 years on. *Carcinogenesis* **40**, 1299–1307 (2019).
22. Tomczak, K., Czerwińska, P. & Wiznerowicz, M. The Cancer Genome Atlas (TCGA): an immeasurable source of knowledge. *Contemp Oncol (Pozn)* **19**, A68–77 (2015).
23. Shimada, K., Muhlich, J.L. & Mitchison, T.J. A tool for browsing the Cancer Dependency Map reveals functional connections between genes and helps predict the efficacy and selectivity of candidate cancer drugs. *bioRxiv*, 2019.2012.2013.874776 (2019).
24. Liberzon, A. *et al.* The Molecular Signatures Database (MSigDB) hallmark gene set collection. *Cell systems* **1**, 417–425 (2015).
25. Thomas, P. D. *et al.* PANTHER: Making genome-scale phylogenetics accessible to all. *Protein Science* **31**, 8–22 (2022).
26. Casella, G. *et al.* Transcriptome signature of cellular senescence. *Nucleic acids research* **47**, 7294–7305 (2019).
27. Hernandez-Segura, A. *et al.* Unmasking Transcriptional Heterogeneity in Senescent Cells. *Current biology: CB* **27**, 2652–2660.e2654 (2017).
28. Nagano, T. *et al.* Identification of cellular senescence-specific genes by comparative transcriptomics. *Scientific reports* **6**, 31758 (2016).
29. Purcell, M., Kruger, A. & Tainsky, M. A. Gene expression profiling of replicative and induced senescence. *Cell cycle (Georgetown, Tex.)* **13**, 3927–3937 (2014).
30. Allen, M. A. *et al.* Global analysis of p53-regulated transcription identifies its direct targets and unexpected regulatory mechanisms. *eLife* **3**, e02200 (2014).

31. Andrysik, Z. *et al*. Identification of a core TP53 transcriptional program with highly distributed tumor suppressive activity. *Genome research* **27**, 1645–1657 (2017).
32. Fischer, M., Steiner, L. & Engeland, K. The transcription factor p53: Not a repressor, solely an activator. *Cell Cycle* **13**, 3037–3058 (2014).
33. Galbraith, M. D., Andrysik, Z., Sullivan, K. D. & Espinosa, J. M. Global Analyses to Identify Direct Transcriptional Targets of p53. *Methods Mol Biol* **2267**, 19–56 (2021).
34. Callari, M. Cancer-specific association between Tau (MAPT) and cellular pathways, clinical outcome, and drug response, *Zenodo*, https://doi.org/10.5281/zenodo.8069665 (2023).
35. Bronkhorst, I. H. G. & Jager, M. J. Inflammation in uveal melanoma. *Eye* **27**, 217–223 (2013).
36. Vernot, J. P. Senescence-Associated Pro-inflammatory Cytokines and Tumor Cell Plasticity. *Front Mol Biosci* **7**, 63 (2020).
37. Xu, W. *et al*. The Genetic Variation of SORCS1 Is Associated with Late-Onset Alzheimer's Disease in Chinese Han Population. *PloS one* **8**, e63621 (2013).
38. Ghosh, A. & Giese, K. P. Calcium/calmodulin-dependent kinase II and Alzheimer's disease. *Molecular Brain* **8**, 78 (2015).
39. Andre, F. *et al*. Microtubule-Associated Protein-tau is a Bifunctional Predictor of Endocrine Sensitivity and Chemotherapy Resistance in Estrogen Receptor–Positive Breast Cancer. *Clinical Cancer Research* **13**, 2061–2067 (2007).
40. Ferreira, A. & Caceres, A. Estrogen-enhanced neurite growth: evidence for a selective induction of Tau and stable microtubules. *The Journal of Neuroscience* **11**, 392–400 (1991).
41. Lew, G. M. Changes in microtubular tau protein after estrogen in a cultured human neuroblastoma cell line. *General Pharmacology: The Vascular System* **24**, 1383–1386 (1993).
42. Bertheau, P. *et al*. p53 in breast cancer subtypes and new insights into response to chemotherapy. *Breast* **22**(Suppl 2), S27–29 (2013).
43. Sola, M. *et al*. Tau protein binds to the P53 E3 ubiquitin ligase MDM2. *Scientific reports* **13**, 10208 (2023).
44. Ard, P. G. *et al*. Transcriptional regulation of the mdm2 oncogene by p53 requires TRRAP acetyltransferase complexes. *Molecular and cellular biology* **22**, 5650–5661 (2002).
45. He, T. *et al*. NMI: a potential biomarker for tumor prognosis and immunotherapy. *Frontiers in pharmacology* **13**, 1047463 (2022).
46. Angel, P.M. & Zambrzycki, S.C. Chapter Two - Predictive value of collagen in cancer, in *Advances in Cancer Research*, Vol. 154. (eds. Angel, P. M. & Ostrowski, M. C.) 15–45 (Academic Press, 2022).
47. Kazerounian, S., Yee, K. O. & Lawler, J. Thrombospondins in cancer. *Cellular and molecular life sciences: CMLS* **65**, 700–712 (2008).
48. Kim, Y. J. *et al*. Suppression of breast cancer progression by FBXL16 via oxygen-independent regulation of HIF1α stability. *Cell reports* **37**, 109996 (2021).
49. Ma, Y. *et al*. PDIA6 promotes pancreatic cancer progression and immune escape through CSN5-mediated deubiquitination of β-catenin and PD-L1. *Neoplasia (New York, N.Y.)* **23**, 912–928 (2021).
50. Theuerkorn, M., Fischer, G. & Schiene-Fischer, C. Prolyl cis/trans isomerase signalling pathways in cancer. *Current opinion in pharmacology* **11**, 281–287 (2011).
51. Sawas, A., Radeski, D. & O'Connor, O. A. Belinostat in patients with refractory or relapsed peripheral T-cell lymphoma: a perspective review. *Therapeutic advances in hematology* **6**, 202–208 (2015).
52. Buxeraud, J. & Faure, S. Le talazoparib (Talzenna®), un inhibiteur de poly(ADP-ribose) polymérase. *Actualités Pharmaceutiques* **61**, 11–12 (2022).
53. Oza, J. *et al*. A phase 2 study of belinostat and SGI-110 (guadecitabine) for the treatment of unresectable and metastatic conventional chondrosarcoma. *Journal of Clinical Oncology* **39**, TPS11578–TPS11578 (2021).
54. Engert, F., Kovac, M., Baumhoer, D., Nathrath, M. & Fulda, S. Osteosarcoma cells with genetic signatures of BRCAness are susceptible to the PARP inhibitor talazoparib alone or in combination with chemotherapeutics. *Oncotarget* **8** (2016).
55. Brandt, J. P. & Gerriets, V. Bleomycin, in *StatPearls* (Treasure Island (FL); 2023).
56. Munster, P. *et al*. First-in-Human Phase I Study of GSK2126458, an Oral Pan-Class I Phosphatidylinositol-3-Kinase Inhibitor, in Patients with Advanced Solid Tumor Malignancies. *Clinical Cancer Research* **22**, 1932–1939 (2016).
57. Sever, R. & Brugge, J.S. Signal transduction in cancer. *Cold Spring Harb Perspect Med* **5** (2015).
58. Waldman, A. D., Fritz, J. M. & Lenardo, M. J. A guide to cancer immunotherapy: from T cell basic science to clinical practice. *Nature Reviews Immunology* **20**, 651–668 (2020).
59. Ospina-Romero, M. *et al*. Association Between Alzheimer Disease and Cancer With Evaluation of Study Biases: A Systematic Review and Meta-analysis. *JAMA network open* **3**, e2025515 (2020).
60. Logotheti, S. *et al*. Neural Networks Recapitulation by Cancer Cells Promotes Disease Progression: A Novel Role of p73 Isoforms in Cancer-Neuronal Crosstalk. *Cancers* **12**, 3789 (2020).
61. Jobling, P. *et al*. Nerve–Cancer Cell Cross-talk: A Novel Promoter of Tumor Progression. *Cancer research* **75**, 1777–1781 (2015).
62. Madeo, M. *et al*. Cancer exosomes induce tumor innervation. *Nature communications* **9**, 4284 (2018).
63. Mancino, M., Ametller, E., Gascón, P. & Almendro, V. The neuronal influence on tumor progression. *Biochimica et Biophysica Acta (BBA) - Reviews on Cancer* **1816**, 105–118 (2011).
64. Neman, J. *et al*. Human breast cancer metastases to the brain display GABAergic properties in the neural niche. *Proceedings of the National Academy of Sciences* **111**, 984–989 (2014).
65. Su, A. *et al*. Malignant Melanoma With Neural Differentiation: An Exceptional Case Report and Brief Review of the Pertinent Literature. *The American Journal of Dermatopathology* **36** (2014).
66. Gargini, R. *et al*. The IDH-TAU-EGFR triad defines the neovascular landscape of diffuse gliomas. *Science translational medicine* **12** (2020).
67. Baquero, M. T. *et al*. Evaluation of prognostic and predictive value of microtubule associated protein tau in two independent cohorts. *Breast Cancer Research* **13**, R85 (2011).
68. Pentheroudakis, G. *et al*. Gene expression of estrogen receptor, progesterone receptor and microtubule-associated protein Tau in high-risk early breast cancer: a quest for molecular predictors of treatment benefit in the context of a Hellenic Cooperative Oncology Group trial. *Breast Cancer Research and Treatment* **116**, 131–143 (2009).
69. Pusztai, L. *et al*. Evaluation of Microtubule-Associated Protein-Tau Expression As a Prognostic and Predictive Marker in the NSABP-B 28 Randomized Clinical Trial. *Journal of Clinical Oncology* **27**, 4287–4292 (2009).
70. Bonneau, C., Gurard-Levin, Z. A., Andre, F., Pusztai, L. & Rouzier, R. Predictive and Prognostic Value of the TauProtein in Breast Cancer. *Anticancer Res* **35**, 5179–5184 (2015).
71. Shao, Y.-Y. *et al*. Predictive and Prognostic Values of Tau and ERCC1 in Advanced Breast Cancer Patients Treated with Paclitaxel and Cisplatin. *Japanese Journal of Clinical Oncology* **40**, 286–293 (2010).
72. Ikeda, H. *et al*. The estrogen receptor influences microtubule-associated protein tau (MAPT) expression and the selective estrogen receptor inhibitor fulvestrant downregulates MAPT and increases the sensitivity to taxane in breast cancer cells. *Breast Cancer Res* **12**, R43 (2010).
73. Morel, M., Shah, K. N. & Long, W. The F-box protein FBXL16 up-regulates the stability of C-MYC oncoprotein by antagonizing the activity of the F-box protein FBW7. *The Journal of biological chemistry* **295**, 7970–7980 (2020).
74. Smoter, M. *et al*. Tau protein as a potential predictive marker in epithelial ovarian cancer patients treated with paclitaxel/platinum first-line chemotherapy. *J Exp Clin Cancer Res* **32**, 25 (2013).
75. Yamauchi, A., Kobayashi, A., Oikiri, H. & Yokoyama, Y. Functional role of the Tau protein in epithelial ovarian cancer cells. *Reprod Med Biol* **16**, 143–151 (2017).

76. Zarin, B. *et al*. A review on the role of tau and stathmin in gastric cancer metastasis. *European Journal of Pharmacology* **908**, 174312 (2021).
77. Sangrajrang, S. *et al*. Estramustine resistance correlates with tau over-expression in human prostatic carcinoma cells. *Int J Cancer* **77**, 626–631 (1998).
78. Yoo, J., Shim, B. Y., Yoo, C. Y., Kang, S. J. & Lee, K. Y. Predictive Significance of KRAS and Tau for Chemoresponse in Advanced Non-Small-Cell Lung Cancer. *J Pathol Transl Med* **43**, 435–440 (2009).
79. Ward, E., DeSantis, C., Robbins, A., Kohler, B. & Jemal, A. Childhood and adolescent cancer statistics, 2014. *CA: A Cancer Journal for Clinicians* **64**, 83–103 (2014).
80. Zhao, Z. *et al*. Aurora B kinase as a novel molecular target for inhibition the growth of osteosarcoma. *Mol Carcinog* **58**, 1056–1067 (2019).
81. Mickymaray, S. *et al*. Rhaponticin suppresses osteosarcoma through the inhibition of PI3K-Akt-mTOR pathway. *Saudi Journal of Biological Sciences* **28**, 3641–3649 (2021).
82. Pérez-Fidalgo, J. A. *et al*. Aurora kinases in ovarian cancer. *ESMO Open* **5**, e000718–e000718 (2020).
83. Han, J. *et al*. MEK inhibitors for the treatment of non-small cell lung cancer. *Journal of Hematology & Oncology* **14**, 1 (2021).
84. Nusinow, D. P. *et al*. Quantitative Proteomics of the Cancer Cell Line Encyclopedia. *Cell* **180**, 387–402.e316 (2020).
85. Chen, E. Y. *et al*. Enrichr: interactive and collaborative HTML5 gene list enrichment analysis tool. *BMC bioinformatics* **14**, 128 (2013).
86. Wilkerson, M. D. & Hayes, D. N. ConsensusClusterPlus: a class discovery tool with confidence assessments and item tracking. *Bioinformatics (Oxford, England)* **26**, 1572–1573 (2010).
87. Thomas, P. D. *et al*. PANTHER: a browsable database of gene products organized by biological function, using curated protein family and subfamily classification. *Nucleic acids research* **31**, 334–341 (2003).
88. Dong, X., Vegesna, K., Brouwer, C. & Luo, W. SBGNview: towards data analysis, integration and visualization on all pathways. *Bioinformatics (Oxford, England)* **38**, 1473–1476 (2022).

Acknowledgements

We thank all members of the Aging Disorders Laboratory for their support and advice during this study. This work was generously supported by the Gelu Foundation, the Mecri Foundation, the Fondazione Ticinese per la Ricerca sul Cancro, and the Gabriele Foundation. Luca Colnaghi gratefully acknowledges support from Vita-Salute San Raffaele University.

Author contributions

Maurizio Callari performed the bioinformatic analysis, collected the data, prepared figures, and contributed to the data interpretation and manuscript writing; Martina Sola and Claudia Magrin contributed to the data interpretation and prepared cell lines and samples for the RNAseq; Andrea Rinaldi produced the cDNA library and performed the RNAseq; Marco Bolis processed and analyzed the RNAseq raw data; Luca Colnaghi contributed to the concept and overview of the study; Paolo Paganetti contributed to the concept and overview of the study and provided the financial support, Stéphanie Papin conceived the study, interpreted the data, and wrote the first manuscript draft. All authors revised the final manuscript version.

Competing interests

The authors declare no competing financial and non-financial interests. No funding organizations were involved in the conceptualization, design, data collection, analysis, decision to publish, preparation of the paper, or may gain or lose financially through this publication. There are no patents, products in development, or marketed products to declare.

Additional information

Supplementary information The online version contains supplementary material available at https://doi.org/10.1038/s41597-023-02543-y.

Correspondence and requests for materials should be addressed to P.P. or L.C.

Reprints and permissions information is available at www.nature.com/reprints.

Publisher's note Springer Nature remains neutral with regard to jurisdictional claims in published maps and institutional affiliations.